ACS APPLIED MATERIALS & INTERFACES

Research Article

www.acsami.org

Extruded Superparamagnetic Saloplastic Polyelectrolyte Nanocomposites

Jingcheng Fu, Qifeng Wang, and Joseph B. Schlenoff*

Department of Chemistry & Biochemistry, The Florida State University, Tallahassee, Florida 32306-4390, United States

Supporting Information

ABSTRACT: Iron oxide nanoparticles of diameter *ca.* 12 nm were dispersed into polyelectrolyte complexes made from poly(styrenesulfonate) and poly(diallyldimethylammonium). These nanocomposites were plasticized with salt water and extruded into dense, tough fibers. Magnetometry of these composites showed they retained the superparamagnetic properties of their constituent nanoparticles with saturation magnetization that scaled with the loading of nanoparticles. Their superparamagnetic response allowed the composites to be heated remotely by radiofrequency fields. While the modulus of fibers was unaffected by the presence of nanoparticles the toughness and tensile strength increased significantly.

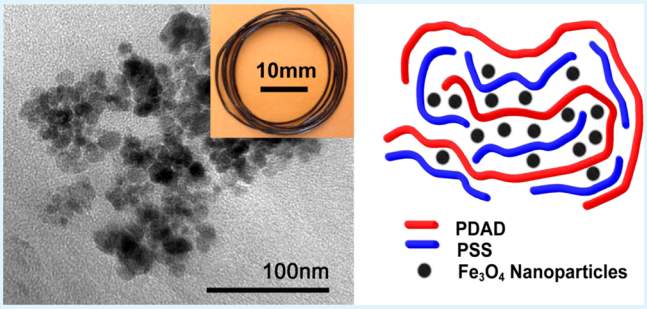

KEYWORDS: *PSS, PDADMA, magnetic nanoparticle, radiofrequency heating, polyelectrolyte complex, SPION*

INTRODUCTION

Many applications for magnetic iron oxide nanoparticles (IONs) have been reported, including targeted drug delivery,[1] biosensors,[2] magnetic resonance imaging contrast agents,[3] data storage,[4] and lithium ion battery anodes.[5] Incorporating nanoparticles into polymers can produce composites with enhanced capabilities. The polymer matrix immobilizes nanoparticles for extended use and protects them from the external environment. For example, dispersing nanoparticles as a composite can enhance their performance as catalysts.[6] Composites made of biocompatible polymer resins have been used for antibacterial applications.[7] Conversely, including nanoparticles can optimize the properties of the host polymer, such as mechanical-to-electrical conversion efficiency.[8]

Magnetic nanoparticle/polymer composites may be shaped into many different forms including thin films: Gass et al. reported spin coating superparamagnetic poly(methyl methacrylate)/polypyrrole bilayers with Fe_3O_4 nanoparticles.[9] Taccola et al. found that poly(3,4-ethylenedioxythiophene):poly(styrenesulfonate) (PEDOT:PSS) ultrathin films with iron oxide nanoparticles can be used as humidity sensors.[10] Polyacrylonitrile/Fe_3O_4 nanocomposite fibers with low bead content can be prepared by electrospinning.[11] Similarly, wet spinning of alginate/Fe_3O_4 yields nanocomposite fibers with potential use as hyperthermia materials.[12] Ultrathin composite films are produced by layer-by-layer assembly.[13]

Bulk methods to make polymer/nanoparticle composites, such as melt blending,[14] in situ polymerization,[15,16] and sol–gel routes,[17,18] face the challenge of minimizing particle aggregation. In situ polymerization consists of mixing nanoparticles with monomer and then polymerizing the latter.[19] Surface pretreatments help the nanoparticles disperse better in the polymer matrix. The sol–gel route, which avoids heating the nanoparticles, yields high-purity composites with better nanoparticle distribution at low temperature.[20]

Polyelectrolyte complexes, PECs, consist of blends of oppositely charged polyelectrolytes. They are made by simple aqueous coprecipitation of components

$$Pol^+Cl^-_{aq} + Pol^-Na^+_{aq} \rightleftharpoons Pol^+Pol^-_p + Cl^-_{aq} + Na^+_{aq} \quad (1)$$

where Pol^+ and Pol^- are polyelectrolyte cation and polyelectrolyte anion repeat units, respectively. The subscript p refers to the PEC phase. We have recently shown that PECs, when plasticized by salt and water, may be efficiently extruded using standard laboratory extruders.[21] It is possible to mix components, such as magnetic particles, with polyelectrolytes to make "saloplastic" materials with specialized properties.[22]

In the present work, we explore straightforward methods of making composites with IONs and PECs. The complexes themselves are biocompatible, as demonstrated by the extensive use of PECs in the "multilayer" format at the biology/materials interface.[23] In addition, the modulus of saloplastics is in the range from 0.1 to 10 MPa, giving them more flexibility than metals or ceramics. Saloplastics thus are suitable for bioimplants and tissue engineering.[24] IONs are incorporated to illustrate blend-extrusion principles and allow the composite to be heated remotely, as might be required to release biologically

Received: October 27, 2014
Accepted: December 8, 2014
Published: December 19, 2014

active molecules trapped in them, or for hyperthermia applications.

The optimal nanocomposite would retain the properties of the host (PEC) and guest (ION) while maintaining good dispersion of the nanoparticle. IONs/polyelectrolyte fluids have been prepared with polyanions, such as poly(styrenesulfonate), PSS,[25] or polycations, such as poly(diallyldimethylammonium), PDADMA.[26] These two polyelectrolytes are excellent materials for saloplastic processing, since their PEC glass transition temperature, T_g, when fully hydrated is in the range of 40−50 °C.[27] Doping with salt decreases this T_g.[27]

EXPERIMENTAL SECTION

Materials. Iron(III) chloride hexahydrate (Alfa Aesar), iron(II) chloride tetrahydrate (Avantor), and ammonium hydroxide (28−30% NH_3 in water, Sigma-Aldrich) were used as received. PSS was supplied by AkzoNobel (VERSA TL130, molecular weight, MW, ca. 200 000 g mol^{-1}) and PDADMAC by Ondeo-Nalco (SD 46104, MW ca. 400 000 g mol^{-1}). Sodium chloride (Aldrich) was used to plasticize polyelectrolyte complexes. Potassium bromide (ACS reagent, ≥99%), hydrochloric acid, hydroxylamine hydrochloride (ACS reagent, 98%), sodium acetate trihydrate (ReagentPlus, ≥99%), 1,10-phenanthroline (≥99%), and sulfuric acid were from Aldrich. Deionized water (Barnstead, E-pure) was used to prepare all solutions.

Nanoparticle Synthesis. Nanoparticles were synthesized following the method developed by Massart.[28] 50 mL of 0.70 M ammonia was added to a mixture of 1.0 mL of ferrous chloride (2.0 M in HCL 2.0 M) and 4.0 mL ferric chloride (1.0 M) under sonication for 30 min.

PSS in 0.25 M NaCl and PDADMAC (without NaCl) solutions were prepared at a concentration of 0.125 M with respect to their monomer units. Nanoparticles were separated from 2.24, 11.2, and 22.4 mL of their suspensions in ammonia using a Nd magnet. Each batch of nanoparticles was then peptized using 100 mL of PDADMA solution, and 1.46 g of NaCl was added. Each 100 mL of PDADMA/nanoparticles suspension was poured simultaneously with 100 mL of PSS solution into a 500 mL beaker with stirring to yield ION-PEC composite loaded with different amounts of nanoparticle. The ION-PEC was then chopped into pieces ca. 8 mm in size and soaked in 1.0 M NaCl for 24 h.[21] Fully hydrated ION-PEC was added into the hopper of a laboratory extruder (Model LE-075 Custom Scientific Instruments). The following parameters were used for extrusion: rotor temperature, 95 °C; header temperature, 96 °C; gap space, 3.8 mm; rotor speed, 110 rpm. A model CSI-194T take-up reel with a 3 cm diameter drum was used to continuously collect the extruded ION-PEC fiber at 10 rpm. PEC without nanoparticles was also prepared by the same method. Dry PECs swell 30−40 vol. % (10−15% in diameter) when immersed in water.[21]

Determination of Iron Content. Approximately 7 mg of each ION-PEC fiber was dried under vac for 24 h at room temperature. ION-PEC fiber, 0.8 ± 0.1 mm diameter, was weighed and submerged in 15 mL of 2.5 M KBr in a vial over a permanent magnet for 24 h to dissolve the complex, whereupon all nanoparticles were collected at the bottom of the vial. The KBr supernate was removed by pipet, and 0.15 mL of 3 M H_2SO_4 was added to the vial to dissolve the nanoparticles. After 24 h, iron was determined following a literature method:[29] 0.1 mL of 10% NH_2OH was added to each vial to neutralize and reduce the iron(III) to iron(II). Then 1 mL of phenanthroline 0.25% (w/v) solution was added to form phenanthroline ferrous complex. A 10% amount of NaOAc was added as a buffer. The absorbance was taken at 510 nm. Calibration curves were made using ferrous sulfate standards.

Measurements. To image the ION-PEC fibers, samples were soaked in DI water and cut into 10 μm thick slices with a cryostat microtome (Leica CM 1850) and imaged with a Nikon Eclipse Ti inverted microscope. ION-PEC fiber was cut into 70 nm slices and mounted on a copper grid. Transmission electron microscopy (TEM) images were obtained with a JEM-ARM200cF at 80 kV.

Magnetic susceptibility measurements on ION-PEC fibers were performed with a superconducting quantum interference device (SQUID)-based magnetometer (Quantum Design). ION-PEC fiber was chopped into 0.5 cm lengths and fixed in a plastic straw with diamagnetic tape. Zero-field-cooled (ZFC) and field-cooled (FC) magnetization curves were recorded.

An induction heating system (Easyheat RHS, Ameritherm Inc., 1 kW) was used to heat ION-PEC samples in a radiofrequency field using a copper coil with three loops of 17.5 mm inner diameter and 28 mm outer diameter. A 0.3 g amount of fiber was wrapped around the tip of an alcohol thermometer and inserted into the middle of the coil. Each fiber was equilibrated for 30 s before the RF field (304.8 A, 351 kHz) was applied. Each fiber was heated 3 times for 450 s. The first heating cycle was considered a "pre-heat" to remove water from fibers, which would affect the heating rate of fibers. The last two heating cycles were used to calculate the initial or maximum heating rate over the first 30 s. The heat generated was estimated using the total heat capacity and temperature rise of the sample and thermometer. Heat capacities were as follows: iron oxide nanoparticles, 0.75 J g^{-1} K^{-1}; polyelectrolyte complexes, 1.5 J g^{-1} K^{-1}; glass of thermometer, 0.84 J g^{-1} K^{-1}; and the liquid in thermometer, 2.0 J g^{-1} K^{-1}.

The equilibrium modulus was tested for all ION-PEC fibers and pure PEC fiber via stress relaxation with a TH2730 (Thümler GmbH) tensile testing unit equipped with 100 N load cell. Residual stress introduced by extrusion was first removed by soaking (annealing) samples in 1 M NaCl for 24 h. Samples were immersed in 0.1 M NaCl during tests to ensure they were fully hydrated. Samples with diameter 1 mm and length 10 mm were elongated to a strain, ε, of 2% at a speed of 5 mm min^{-1} (50% strain per minute), and the relaxation of the stress was recorded. Equilibrium stress, σ_0, was obtained when stress vs time reached a plateau. The equilibrium modulus is determined by $E_0 = \sigma_0/\varepsilon$.

Strain to break tests at a speed of 5 mm min^{-1} were performed using annealed samples immersed in 0.1 M NaCl.[30,31] True strength, σ, and true strain, ε, were calculated as

$$\varepsilon = \ln\left(\frac{L}{L_o}\right) \quad \sigma = \frac{FL}{A_o L_o} \tag{2}$$

where L is the instantaneous length of the fiber, L_0 is the original length, F is the force, and A_0 is the original cross section area of the fiber. Toughness (U) of the fiber was calculated by integrating the area under the stress−strain curve.

RESULTS AND DISCUSSION

Imbedding Nanoparticles in PEC. PSS/PDADMA polyelectrolyte complex was obtained by mixing the respective solutions, Scheme 1.[21] Efficient blending of polymer components is driven by ion pairing between charged repeat units.[32] In the present case, the challenge is to optimize the dispersion of the third component, the nanoparticles, within the polyelectrolyte matrix.

Scheme 1. Two-Step Mixing Procedure To Make ION-PEC

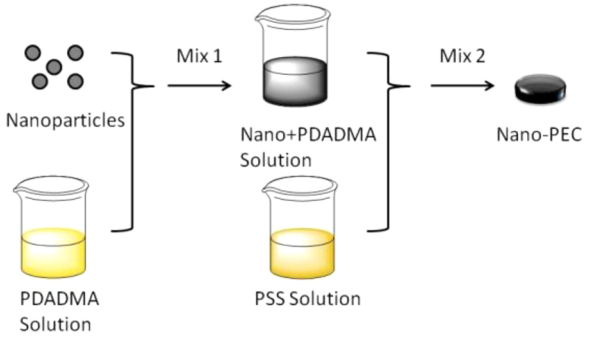

dx.doi.org/10.1021/am5074694 | ACS Appl. Mater. Interfaces 2015, 7, 895−901

Figure 1. Images of extruded ION-PEC fibers. (Left to right) Nanoparticle contents are 0.5%, 2.1%, and 4.5% by weight.

Dispersions of iron oxide nanoparticles in solution require electrostatic stabilization at high pH or low pH, since the pK_a of the Fe_3O_4 surface is close to 7.[33,34] Under the basic solution conditions (ammonia) employed for synthesis the surface will be negatively charged. Initially it was believed that IONs would interact with and be precipitated by PDADMA but remain stable in PSS. A number of trials with different polymers, concentrations, and molecular weights showed the IONs were, in fact, the most stable (against precipitation) in solutions of 0.125 M PDADMA. This result is reasonable, given the structural similarity of PDADMA to the tetraalkylammonium ions often used to stabilize (peptize) IONs at high pH.[35]

Also, unexpectedly, it was discovered that PDADMAC with "high" molecular weight (MW ca. 400 000) was better at stabilizing IONS than either "medium" (200 000−300 000) or "low" MW (100 000−200 000). Because NaCl also destabilized ION dispersions no salt was added to PDADMA solutions, while they were mixed with IONs. Instead, the appropriate salt concentration was added immediately before mixing with PSS.

Morphology. ION-PEC fibers of diameter 1.1 ± 0.2 mm containing 0.5, 2.1, and 4.5 wt % iron oxide loading, as determined from the phenanthroline colorimetric assay, prepared by extrusion are shown in Figure 1. The higher % ION samples were black, consistent with the color of Fe_3O_4,[36] while the reddish color (normally associated with maghemite, γFe_2O_3) seen in the 0.5% sample comes from the pale yellow color of the PEC itself. The color of the fiber did not change for 6 months in ambient, suggesting the magnetite nanoparticles were stable in PEC fibers and were not oxidized to maghemite. Fibers were sectioned for optical and electron microscopy. Figure 2 shows optical micrographs of cross sections. On a millimeter scale the ION was well dispersed, but on the 10 μm scale seen in Figure 2 evidence of clustering is apparent. Localized aggregation of IONs is clearly seen on a 100 nm scale in the TEM image in Figure 3. The diameter of the nanoparticles was 11.6 ± 2.7 nm, in agreement with the diameter of IONs made with the Massart method.[37,38] Though partially aggregated, the IONs still exhibited superparamagnetic behavior equivalent to separated particles (see magnetic characterization below). The TEM in Figure 3 indicates a defect-free interface between the host polymer and the nanoparticles.

Magnetic Properties. Zero-field-cooling (ZFC) and field-cooling (FC) magnetization curves for ION-PECS were obtained with a SQUID at 100 Oe from 1.8 to 400 K. ION-PECs with different loadings of ION behaved similarly, with a blocking temperature (below which samples are ferri- or ferromagnetic) of around 270 K. Figure 4 shows the ZFC and FC curve of 2.1% ION-PEC fiber. Similar magnetization curves and blocking temperature have been observed for Fe_3O_4 IONs of the same size well dispersed in polypyrrole.[9]

The nature of the magnetism in the nanocomposites was characterized via magnetization vs field strength ($M-H$) scans at 300 K over the range from −20 to +20 kOe. Figure 5A and 5B shows $M-H$ curves before and after data were corrected by the nanoparticle weight percentage. Figure 5A indicates that all of the three PECs are close to their saturation magnetization values, M_s, at extremes of applied field, and those with greater nanoparticle content have higher M_s. The ratio of the M_s of the three loadings is 1:4.5:8.9, consist with the ratio of the nanoparticle content 1:4.2:9, which means the magnetizations, when normalized for weight loading of IONs (Figure 5B), are similar (54.5, 61.4, and 54.4 emu g^{-1} for 0.5, 2.1, and 4.5 wt % ION-PECs, respectively). These values are close to an M_s of ca. 60 emu g^{-1} of Fe_3O_4 nanoparticles with similar size at 300 K.[39]

The slightly lower M_s values in the three samples, compared to M_s limiting values (60−70 emu g^{-1}) for magnetite nanoparticles with diameters less than 20 nm,[40] can be partially explained by the (diamagnetic) contribution of the polymer matrix. This is especially noticeable for the ION-PEC with the lowest loading, which leads to a negative slope at high H. The near-zero coercivity, typical of the superparamagnetic behavior of IONs, remained in all ION-PEC nanocomposites (coercivities $\leq$ 20 Oe of 15.00, 15.07, and 11.47 Oe or 0.5, 2.1, and 4.5 wt %) as shown in Figures 6 and S1, Supporting Information.

Radiofrequency Field Heating. For practical applications this nanocomposite has the potential to be heated by remotely applying a radiofrequency (RF) field.[41] The ability for remote heating would be useful in applications of the composite in drug carriers or implants which release their payload on heating.[42,43] When swollen by water and salt polyelectrolyte complexes are plasticized.[44] The glass transition temperature for PSS/PDADMA PEC in 0.15 M NaCl (i.e., physiological

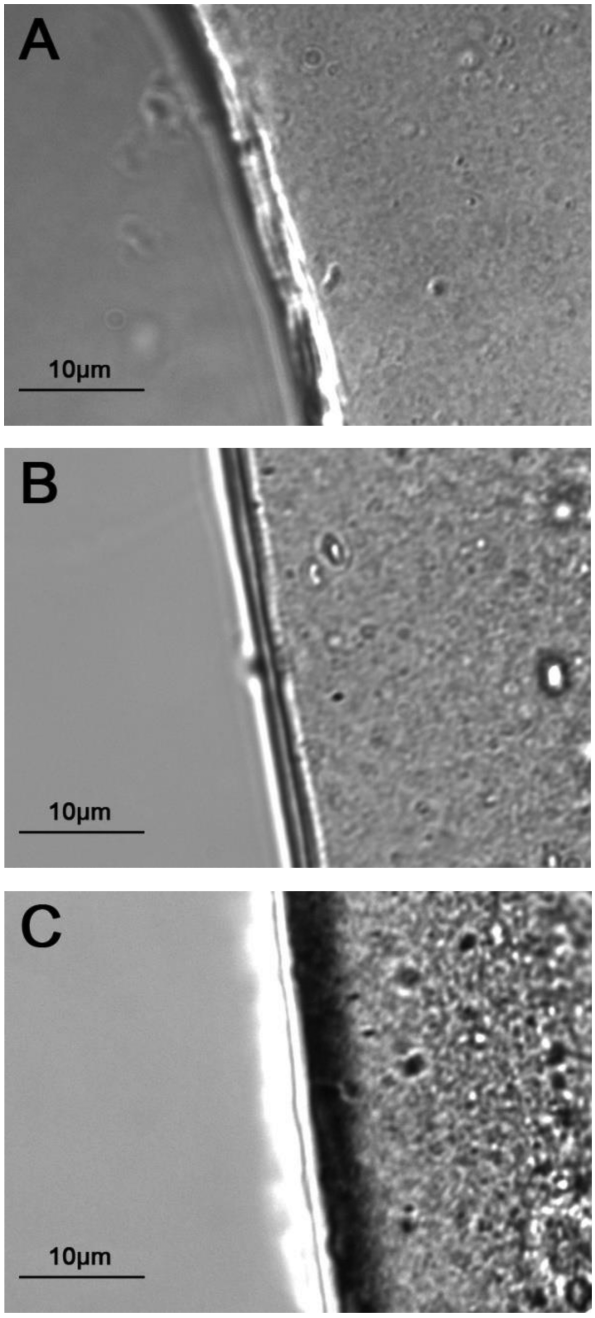

Figure 2. Optical micrographs of cross sections of ION-PEC fibers of 0.5 (A), 2.1 (B), and 4.5 wt % ION (C). The thickness of the slices is 10 μm.

conditions) is slightly above room temperature.[27] Transport through PSS/PDADMA is strongly temperature dependent.[45] Therefore, release by external RF heating of a drug captured within the hydrated ION-PEC is possible.

ION-PEC fibers were heated by inserting them into the coil of an induction heating system operating at a field strength of ca. 40 000 A m^{-1} and a frequency of 351 kHz. Feasibility tests were performed on dry samples since the water content and heat transport rates depend on the surroundings of the composite. Each fiber was heated three times following the same procedure. The temperature−time heating curves of all 3 cycles for 2.1% ION-PEC fiber are shown in the Supporting Information, Figure S2. Compared to the first trial, the second and third trials had identical heating curves with higher

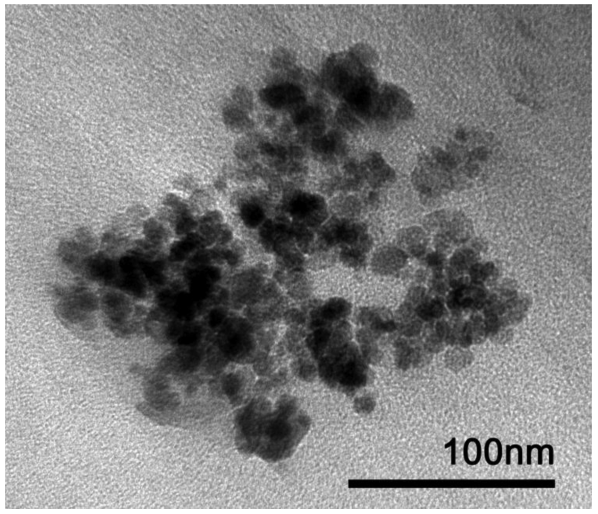

Figure 3. TEM image of the cross section of 2.1% ION-PEC fibers.

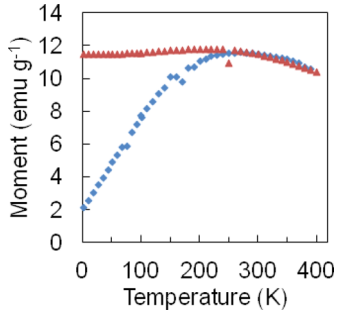

Figure 4. Zero-field-cooled (♦) and field -cooled (▲) magnetic moment versus temperature at 100 Oe for ION-PEC fibers with 2.1 wt % IONs.

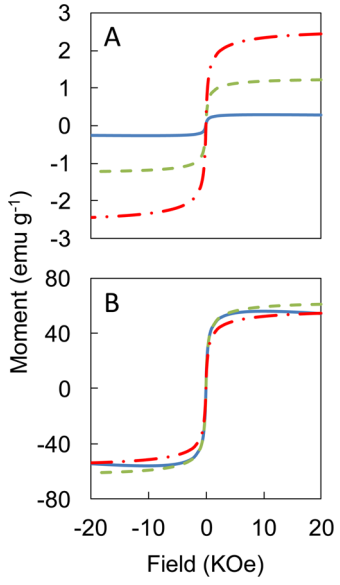

Figure 5. *M*−*H* curve for the ION-PEC fibers based on the weight of the composite (A) and Fe_3O_4 nanoparticles (B): 0.5 (solid line), 2.1 (dashed line) and 4.5 (dash and dot line) wt % at 300 K.

maximum temperatures and initial heating rates, showing that the first heating drove off water and reduced the heat capacity. The maximum temperature attained by the 2.1% fiber was 70 °C for both second and third heating trials, while it was 65.5 °C

dx.doi.org/10.1021/am5074694 | ACS Appl. Mater. Interfaces 2015, 7, 895−901

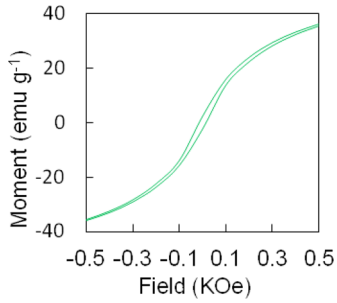

Figure 6. Magnification of the $M-H$ curve near zero field of 2.1% Fe_3O_4 ION-PEC fiber.

for the first heat trial. The initial heating rate was calculated by taking the slope of the linear part of the curve over the first 30 s. The heating rate was 0.3 °C s^{-1} for the second and third trials, while it was 0.2 °C s^{-1} for the first trial. Thus, for each fiber, the first heating was considered a "preheat", and data from the second and third trials were averaged and compared.

Heating curves for the three loadings of IONs under the same conditions are shown in Figure 7, along with a control

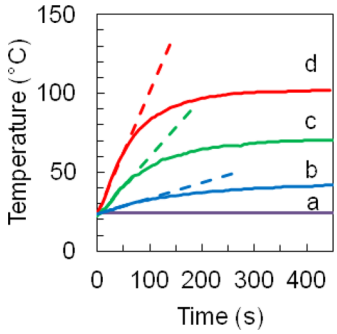

Figure 7. Temperature versus time for ION-PEC fibers containing (a) 0.0%, (b) 0.5%, (c) 2.1%, and (d) 4.5% ION exposed to 1 kW RF field.

(containing no IONs). All nanocomposites showed a relatively steep heating slope followed by a plateau from steady-state transport of heat energy away from the fiber. The control with no IONs showed no temperature change. All ION-PECs approached their maximum temperature (T_m) within 450 s. For 0.5%, 2.1%, and 4.5% nano-PEC fiber the T_m was 42, 71, and 102 °C and the initial heat rates within the first 60 s were 0.1, 0.3, and 0.7 °C s^{-1}, respectively. Thus, both the heating rate and the ultimate steady-state temperature may be tuned by the ION content of the nanocomposite.

The initial power produced for each fiber during RF irradiation was estimated from the temperature change and heat capacities as described in the Experimental Section. The initial slopes in Figure 7 translate to heating powers of 0.39, 1.15, and 2.68 W per gram of composite in each sample of ION-PEC fiber with 0.5%, 2.1%, and 4.5% nanoparticle content, respectively.

Mechanical Properties. The equilibrium modulus for all fibers immersed in 0.10 M NaCl was tested using strain relaxation (raw data in Figure S3, Supporting Information). Fibers with different nanoparticle content were strained rapidly to 2% of the fiber length (within the liner viscoelastic range), and the stress was allowed to relax over the course of a few minutes to steady-state ("equilibrium") values. Using several samples of each ION loading it was determined that the fiber equilibrium modulus was 5 ± 2 MPa with no statistically significant difference between different loadings of ION. Given the low wt % loadings of IONs, which translate to correspondingly smaller volume % (0.1%, 0.5%, and 1% for the three samples), there is no reason to expect a significant dependence of modulus on ION loading.

The toughness of nanocomposites was measured, while they were immersed in 0.1 M NaCl, which is the salt concentration at which we found PSS/PDADMA PECs to have maximum toughness.[21] ION-PEC fibers were strained to break in 0.1 M NaCl after they were conditioned in this same electrolyte for 24 h. True stress vs true strain curves for ION-PEC fibers and a control without nanoparticles are shown in Figure 8. The

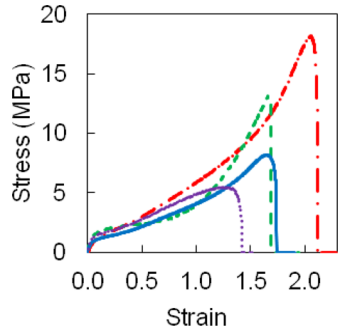

Figure 8. Strain to break test for nano-PEC fiber immersed in 0.1 M NaCl solution for 24 h using true stress and true strain for 0 (dotted line), 0.5 (solid line), 2.1 (dashed line), and 4.5 (dash–dot line) wt % IONs.

stress–strain response is similar for all PECs, with an initial higher modulus in the linear viscoelastic regime followed by a long plastic deformation. Toughness was obtained from the area under the curves. Toughness and tensile strength are compared in Figure 9. Fibers with nanoparticles showed better ductility and thus better toughness and tensile strength than those without nanoparticles.

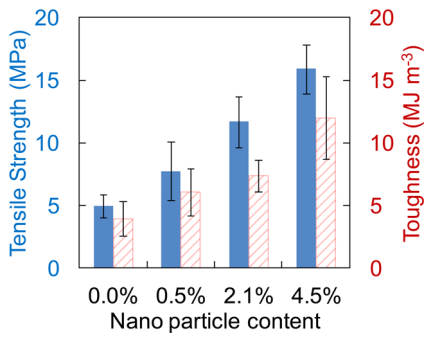

Figure 9. Tensile strength (solid columns) and toughness (striped column) of ION-PEC nanocomposite fibers from Figure 8. Error bars are ±1 standard deviation.

While the toughness of the ION-free PEC fibers was good, the significant (3-fold) improvement in toughness with addition of a small amount of ION was unanticipated. Within the nanocomposite, the well-blended polyelectrolyte components PSS and PDADMA clearly make up the continuous phase. For effective toughening, IONs or their aggregates must relieve or absorb the stress at failure points as the material is starting to reach its limit of extension. With the right kind of matrix/

dx.doi.org/10.1021/am5074694 | ACS Appl. Mater. Interfaces 2015, 7, 895–901

particle interface, nanoparticles are known to behave as a stress "transformer," taking up the majority of force applied on the composite and lowering the force on the continuous phase.[46] Since Fe_3O_4 nanoparticles are much tougher than the base polymer, ION-PEC fibers are able to tolerate more stress and absorb more energy before they break. Good interfacial interactions between nanoparticles and polymer are essential to improving the tensile strength.[47] Interfacial adhesion is required to transfer stress from polymer matrix to inorganic nanoparticle, NP

Our result indicates that PDADMA interacts well with the IONs without additional functionalization (again perhaps a consequence of strong adsorption of tetraalkylammonium onto ION). As an example of NP-induced toughening, it was reported that the tensile strength of polyamide-6 polymer increased 55% with addition of only 4.2 wt % of exfoliated montmorillonite nanoclay.[46] Ou et al. found that the mechanical properties, such as tensile strength, of nylon-6 reached their maximum values when loaded with 5 wt % of silica NPs.[48] Similarly, Xie et al. found that an optimal tensile strength of poly(vinyl chloride)/calcium carbonate ($CaCO_3$) nanocomposite was achieved at 5 wt % of $CaCO_3$.[49] Although the loading of IONs for optimal toughness was not determined here, it may be that 4.5 wt % is close to optimum.

CONCLUSIONS

Though they were dispersed throughout the PEC, the aggregation of IONs was observed on a nanometer scale. This level of aggregation impacted neither the superparamagnetic properties nor the RF-induced heating of the nanocomposite. The processing conditions (elevated temperature and salt concentration) under which ION-PEC composites were extruded into fibers also did not measurably change the properties of the IONs. The temperature rise caused by an external RF field was sufficient to take the hydrated material through its glass transition temperature, which would result in much faster transport of small molecules through the PEC.[45] This strong temperature dependence of molecular diffusion makes ION-PECs good candidates for externally activated carriers for drug release.

ASSOCIATED CONTENT

Supporting Information

Further details on the $M-H$ curve near zero field for the rest of the composites, repeating experiment on heat and time relationships, and stress relaxation for each composite; video of heating composites to break using RF. This material is available free of charge via the Internet at http://pubs.acs.org.

AUTHOR INFORMATION

Corresponding Author

*E-mail: schlen@chem.fsu.edu.

Notes

The authors declare no competing financial interest.

ACKNOWLEDGMENTS

This work was supported by a grant from the National Science Foundation (DMR-1208188). The authors acknowledge assistance from Jared Kinyon for the magnetometry and Yi-Feng Su for the TEM work.

REFERENCES

(1) Sahoo, B.; Devi, K. S. P.; Banerjee, R.; Maiti, T. K.; Pramanik, P.; Dhara, D. Thermal and pH Responsive Polymer-Tethered Multifunctional Magnetic Nanoparticles for Targeted Delivery of Anticancer Drug. *ACS Appl. Mater. Interfaces* **2013**, *5*, 3884−3893.

(2) Pal, S.; Alocilja, E. C. Electrically Active Magnetic Nanoparticles as Novel Concentrator and Electrochemical Redox Transducer in Bacillus Anthracis DNA Detection. *Biosens. Bioelectron.* **2010**, *26*, 1624−1630.

(3) Wang, J. X.; Huang, Y. Z.; David, A. E.; Chertok, B.; Zhang, L.; Yu, F. Q.; Yang, V. C. Magnetic Nanoparticles for MRI of Brain Tumors. *Curr. Pharm. Biotechnol.* **2012**, *13*, 2403−2416.

(4) Sun, S. H. Recent Advances in Chemical Synthesis, Self-Assembly, and Applications of FePt Nanoparticles. *Adv. Mater.* **2006**, *18*, 393−403.

(5) Chen, D. Y.; Ji, G.; Ma, Y.; Lee, J. Y.; Lu, J. M. Graphene-Encapsulated Hollow Fe_3O_4 Nanoparticle Aggregates as a High-Performance Anode Material for Lithium Ion Batteries. *ACS Appl. Mater. Interfaces* **2011**, *3*, 3078−3083.

(6) Pan, X.; Zhao, Y.; Liu, S.; Korzeniewski, C. L.; Wang, S.; Fan, Z. Y. Comparing Graphene-TiO_2 Nanowire and Graphene-TiO_2 Nanoparticle Composite Photocatalysts. *ACS Appl. Mater. Interfaces* **2012**, *4*, 3944−3950.

(7) Mallick, S.; Sharma, S.; Banerjee, M.; Ghosh, S. S.; Chattopadhyay, A.; Paul, A. Iodine-Stabilized Cu Nanoparticle Chitosan Composite for Antibacterial Applications. *ACS Appl. Mater. Interfaces* **2012**, *4*, 1313−1323.

(8) Kim, K.; Zhu, W.; Qu, X.; Aaronson, C.; McCall, W. R.; Chen, S.; Sirbuly, D. J. 3D Optical Printing of Piezoelectric Nanoparticle−Polymer Composite Materials. *ACS Nano* **2014**, *8*, 9799−9806.

(9) Gas, J.; Poddar, P.; Almand, J.; Srinath, S.; Srikanth, H. Superparamagnetic Polymer Nanocomposites with Uniform Fe_3O_4 Nanoparticle Dispersions. *Adv. Funct. Mater.* **2006**, *16*, 71−75.

(10) Taccola, S.; Greco, F.; Zucca, A.; Innocenti, C.; Fernandez, C. D.; Campo, G.; Sangregorio, C.; Mazzolai, B.; Mattoli, V. Characterization of Free-Standing PEDOT:PSS/Iron Oxide Nanoparticle Composite Thin Films and Application as Conformable Humidity Sensors. *ACS Appl. Mater. Interfaces* **2013**, *5*, 6324−6332.

(11) Zhang, D.; Karki, A. B.; Rutman, D.; Young, D. R.; Wang, A.; Cocke, D.; Ho, T. H.; Guo, Z. H. Electrospun Polyacrylonitrile Nanocomposite Fibers Reinforced with Fe_3O_4 Nanoparticles: Fabrication and Property Analysis. *Polymer* **2009**, *50*, 4189−4198.

(12) Stone, R.; Hipp, S.; Barden, J.; Brown, P. J.; Mefford, O. T. Highly Scalable Nanoparticle-Polymer Composite Fiber Via Wet Spinning. *J. Appl. Polym. Sci.* **2013**, *130*, 1975−1980.

(13) Pichon, B. P.; Louet, P.; Felix, O.; Drillon, M.; Begin-Colin, S.; Decher, G. Magnetotunable Hybrid Films of Stratified Iron Oxide Nanoparticles Assembled by the Layer-by-Layer Technique. *Chem. Mater.* **2011**, *23*, 3668−3675.

(14) Biswas, S.; Belfield, K. D.; Das, R. K.; Ghosh, S.; Hebard, A. F. Block Copolymer-Mediated Formation of Superparamagnetic Nanocomposites. *Chem. Mater.* **2009**, *21*, 5644−5653.

(15) Shirali, H.; Rafizadeh, M.; Taromi, F. A. Synthesis and Characterization of Amorphous and Impermeable Poly(Ethylene-Co-1,4cyclohexylenedimethylene Terephthalate)/Organoclay Nanocomposite Via in Situ Polymerization. *J. Compos. Mater.* **2014**, *48*, 301−315.

(16) Park, C.; Ounaies, Z.; Watson, K. A.; Crooks, R. E.; Smith, J.; Lowther, S. E.; Connell, J. W.; Siochi, E. J.; Harrison, J. S.; Clair, T. L. S. Dispersion of Single Wall Carbon Nanotubes by in Situ Polymerization under Sonication. *Chem. Phys. Lett.* **2002**, *364*, 303−308.

(17) Zhang, F.; Zhang, W.; Yu, Y.; Deng, B.; Li, J.; Jin, J. Sol−Gel Preparation of PAA-G-PVDF/TiO_2 Nanocomposite Hollow Fiber Membranes with Extremely High Water Flux and Improved Antifouling Property. *J. Membr. Sci.* **2013**, *432*, 25−32.

(18) Wen, J. Y.; Wilkes, G. L. Organic/Inorganic Hybrid Network Materials by the Sol-Gel Approach. *Chem. Mater.* **1996**, *8*, 1667−1681.

(19) Yang, C. H.; Du, J. J.; Peng, Q.; Qiao, R. R.; Chen, W.; Xu, C.; Shuai, Z. G.; Gao, M. Y. Polyaniline/Fe_3O_4 Nanoparticle Composite: Synthesis and Reaction Mechanism. *J. Phys. Chem. B* **2009**, *113*, 5052−5058.
(20) Luo, M. L.; Tang, W.; Zhao, J. Q.; Pu, C. S. Hydrophilic Modification of Poly(Ether Sulfone) Used TiO_2 Nanoparticles by a Sol-Gel Process. *J. Mater. Process. Technol.* **2006**, *172*, 431−436.
(21) Shamoun, R. F.; Reisch, A.; Schlenoff, J. B. Extruded Saloplastic Polyelectrolyte Complexes. *Adv. Funct. Mater.* **2012**, *22*, 1923−1931.
(22) Tirado, P.; Reisch, A.; Roger, E.; Boulmedais, F.; Jierry, L.; Lavalle, P.; Voegel, J. C.; Schaaf, P.; Schlenoff, J. B.; Frisch, B. Catalytic Saloplastics: Alkaline Phosphatase Immobilized and Stabilized in Compacted Polyelectrolyte Complexes. *Adv. Funct. Mater.* **2013**, *23*, 4785−4792.
(23) Gribova, V.; Auzely-Velty, R.; Picart, C. Polyelectrolyte Multilayer Assemblies on Materials Surfaces: From Cell Adhesion to Tissue Engineering. *Chem. Mater.* **2012**, *24*, 854−869.
(24) Hariri, H. H.; Schlenoff, J. B. Saloplastic Macroporous Polyelectrolyte Complexes: Cartilage Mimics. *Macromolecules* **2010**, *43*, 8656−8663.
(25) Corr, S. A.; Gun'ko, Y. K.; Tekoriute, R.; Meledandri, C. J.; Brougham, D. F. Poly(Sodium-4-Styrene)Sulfonate - Iron Oxide Nanocomposite Dispersions with Controlled Magnetic Resonance Properties. *J. Phys. Chem. C* **2008**, *112*, 13324−13327.
(26) Marangoni, V. S.; Martins, M. V. A.; Souza, J. A.; Oliveira, O. N.; Zucolotto, V.; Crespilho, F. N. The Processing of Polyelectrolyte-Covered Magnetite Nanoparticles in the Form of Nanostructured Thin Films. *J. Nanopart. Res.* **2012**, 14.
(27) Shamoun, R. F.; Hariri, H. H.; Ghostine, R. A.; Schlenoff, J. B. Thermal Transformations in Extruded Saloplastic Polyelectrolyte Complexes. *Macromolecules* **2012**, *45*, 9759−9767.
(28) Massart, R. Preparation of Aqueous Magnetic Liquids in Alkaline and Acidic Media. *IEEE Trans. Magn.* **1981**, *17*, 1247−1248.
(29) Skoog, D. A.; West, D. M.; Holler, J. F.; Crouch, S. R. *Fundamentals of Analytical Chemistry*, 8th ed.; Thomson, Brooks, Cole; Belmont, CA, 2004.
(30) Nicholson, J. W. *The Chemistry of Polymers*, 3rd ed; RSC Pub.: Cambridge, 2006.
(31) Billmeyer, F. W. *Textbook of Polymer Science*, 3rd ed; Wiley: New York, 1984.
(32) Michaels, A. S. Polyelectrolyte Complexes. *Ind. Eng. Chem.* **1965**, *57*, 32−40.
(33) Bacri, J. C.; Perzynski, R.; Salin, D.; Cabuil, V.; Massart, R. Ionic Ferrofluids - a Crossing of Chemistry and Physics. *J. Magn. Magn. Mater.* **1990**, *85*, 27−32.
(34) Laurent, S.; Forge, D.; Port, M.; Roch, A.; Robic, C.; Elst, L. V.; Muller, R. N. Magnetic Iron Oxide Nanoparticles: Synthesis, Stabilization, Vectorization, Physicochemical Characterizations, and Biological Applications. *Chem. Rev.* **2008**, *108*, 2064−2110.
(35) Lu, Z. Y.; Wang, G.; Zhuang, J. Q.; Yang, W. S. Effects of the Concentration of Tetramethylammonium Hydroxide Peptizer on the Synthesis of Fe_3O_4/SiO_2 Core/Shell Nanoparticles. *Colloids Surf. A: Physicochem. Eng. Aspects* **2006**, *278*, 140−143.
(36) Hai, H. T.; Kura, H.; Takahashi, M.; Ogawa, T. Facile Synthesis of Fe_3O_4 Nanoparticles by Reduction Phase Transformation from Gamma-Fe_2O_3 Nanoparticles in Organic Solvent. *J. Colloid Interface Sci.* **2010**, *341*, 194−199.
(37) Sun, M. M.; Zhu, A. M.; Zhang, Q. G.; Liu, Q. L. A Facile Strategy to Synthesize Monodisperse Superparamagnetic OA-Modified Fe_3O_4 Nanoparticles with PEG Assistant. *J. Magn. Magn. Mater.* **2014**, *369*, 49−54.
(38) Cheng, F. Y.; Su, C. H.; Yang, Y. S.; Yeh, C. S.; Tsai, C. Y.; Wu, C. L.; Wu, M. T.; Shieh, D. B. Characterization of Aqueous Dispersions of Fe_3O_4 Nanoparticles and Their Biomedical Applications. *Biomaterials* **2005**, *26*, 729−738.
(39) Goya, G. F.; Berquo, T. S.; Fonseca, F. C.; Morales, M. P. Static and Dynamic Magnetic Properties of Spherical Magnetite Nanoparticles. *J. Appl. Phys.* **2003**, *94*, 3520−3528.
(40) Harris, L. A.; Goff, J. D.; Carmichael, A. Y.; Riffle, J. S.; Harburn, J. J., St; Pierre, T. G.; Saunders, M. Magnetite Nanoparticle Dispersions Stabilized with Triblock Copolymers. *Chem. Mater.* **2003**, *15*, 1367−1377.
(41) Mustafa, T.; Zhang, Y. B.; Watanabe, F.; Karmakar, A.; Asar, M. P.; Little, R.; Hudson, M. K.; Xu, Y.; Biris, A. S. Iron Oxide Nanoparticle-Based Radio-Frequency Thermotherapy for Human Breast Adenocarcinoma Cancer Cells. *Biomater. Sci.* **2013**, *1*, 870−880.
(42) Staruch, R. M.; Ganguly, M.; Tannock, I. F.; Hynynen, K.; Chopra, R. Enhanced Drug Delivery in Rabbit VX2 Tumours Using Thermosensitive Liposomes and MRI-Controlled Focused Ultrasound Hyperthermia. *Int. J. Hyperthermia* **2012**, *28*, 776−787.
(43) Rovers, S. A.; Hoogenboom, R.; Kemmere, M. F.; Keurentjes, J. T. F. Repetitive on-Demand Drug Release by Magnetic Heating of Iron Oxide Containing Polymeric Implants. *Soft Matter* **2012**, *8*, 1623−1627.
(44) Hariri, H. H.; Lehaf, A. M.; Schlenoff, J. B. Mechanical Properties of Osmotically Stressed Polyelectrolyte Complexes and Multilayers: Water as a Plasticizer. *Macromolecules* **2012**, *45*, 9364−9372.
(45) Ghostine, R. A.; Schlenoff, J. B. Ion Diffusion Coefficients through Polyelectrolyte Multilayers: Temperature and Charge Dependence. *Langmuir* **2011**, *27*, 8241−8247.
(46) Mallick, P. *Fiber-Reinforced Composites: Materials, Manufacturing, and Design*, 3rd ed; CRC Press: New York, 2007.
(47) Gu, H. B.; Tadakamalla, S.; Huang, Y. D.; Coloradc, H. A.; Luo, Z. P.; Haldolaarachchige, N.; Young, D. P.; Wei, S. Y.; Guo, Z. H. Polyaniline Stabilized Magnetite Nanoparticle Reinforced Epoxy Nanocomposites. *ACS Appl. Mater. Interfaces* **2012**, *4*, 5613−5624.
(48) Ou, Y. C.; Yang, F.; Yu, Z. Z. New Conception on the Toughness of Nylon 6/Silica Nanocomposite Prepared Via in Situ Polymerization. *J. Polym. Sci., Part B: Polym. Phys.* **1998**, *36*, 789−795.
(49) Xie, X. L.; Liu, Q. X.; Li, R. K. Y.; Zhou, X. P.; Zhang, Q. X.; Yu, Z. Z.; Mai, Y. W. Rheological and Mechanical Properties of PVC/$CaCO_3$ Nanocomposites Prepared by in Situ Polymerization. *Polymer* **2004**, *45*, 6665−6673.